Jurnal Elektronika dan Telekomunikasi (JET), Vol. 23, No. 1, August 2023, pp. 29-36
Accredited by KEMDIKBUDRISTEK, Decree No: **158/E/KPT/2021**
doi: 10.55981/jet.524

Compact Coplanar Waveguide Antenna Using Arm Patch for Software Defined Radio

Nurul Fahmi Arief Hakim*, Silmi Ath Thahirah Al Azhima, Mariya Al Qibtiya

Department of Electrical Engineering Education
Universitas Pendidikan Indonesia
Jalan Dr Setiabudhi No 229
Bandung, Indonesia

Abstract

This article proposes a compact coplanar waveguide (CPW) antenna with a semicircular patch and patch arm above the feed line. The method used in this antenna research is experimental, with antenna parameter optimization, fabrication, and measurement steps. The antenna was 40 mm × 46 mm × 0.8 mm and was printed on an FR4 substrate. Antenna optimization was carried out with CST Studio Suite to obtain optimal results. Based on return loss measurement results, the proposed antenna has an operational frequency of 2 GHz–7 GHz. The antenna arm has a significant effect on the operational frequency of the antenna, as proven by a parameter study of the antenna arm. Parametric studies were carried out on the antenna by investigating the influence of geometric parameters on the frequency characteristics. Optimization results were printed then measured by a Vector Network Analyzer (VNA) and a spectrum analyzer. The fabricated CPW antenna has a wider operating frequency than the simulation. An omnidirectional radiation pattern was observed at 2 GHz–4 GHz. The antenna has been used as a transmitter and receiver at 2.4 GHz, 3 GHz, and 4 GHz. The antenna is able to receive the signal emitted from the signal generator.

Keywords: Antenna, CPW, Software-Defined Radio (SDR), UWB.

I. INTRODUCTION

Wireless communication systems are ever-evolving [1]. The antenna as a medium for transmitting EM waves has been modified to get results according to user specifications [2]. Among various developed antennas, the printed circuit board (PCB) antenna is a readily modified antenna [3], also operable in microwave frequencies. The small dimensions of the antenna make this antenna suitable for use in software-defined radio (SDR). Besides software-defined radio (SDR), this PCB antenna has also been applied to WLAN, satellites, 5G, and others [4]–[7]. The PCB antenna has a narrow operational frequency. However, some modification techniques can change the operating frequency to UWB [8].

One of the applications of telecommunications systems using broadband antennas is software-defined radio (SDR). SDR technology provides a flexible and cost-effective solution to drive communications with broad-reach benefits for users [9]. SDR can enable hardware radios with radio software, supporting more functions integrated into radio sets [10]. Joseph Mitola invented and introduced the SDR in the early 90s as a radio device that is programmable and configurable using the software. GNURadio is open-source-based software that can be used to design and integrate systems with hardware. GNURadio implements the programming language C ++ or Python [11]. In addition to being open-source, GNURadio users can create block diagrams according to the desired specifications. Applications for GNURadio include spectrum measurement, communication systems, and DVB [12]–[14]. SDR is an innovation in radio systems because it can be used for various applications with only one device, such as signal processing, modulation/demodulation, and passive receiver [15]. In addition, SDR can be used to create a new system without replacing or adding its constituent components. Configure the SDR using the software, then loaded into the DSP. One type of SDR called HackRF has an operating frequency of up to 6 GHz. SDR requires an omnidirectional antenna with a frequency of up to 6 GHz to transmit or receive signals, so the antenna frequency and specification must be appropriate for the SDR [16].

Printed circuit board (PCB) antennas have been described in detail in the literature [17], [18]. Lightweight, affordable, conformal, low-profile, and suitable with integrated circuits is just a few features of PCB antennas. Common feeding methods employing transmission lines [19], coupled apertures [20]–[22], or electromagnetic [23], [24], coplanar waveguides [25]–[27], and coaxial probes [28], [29]. Due to their uniplanar implementation and development of vias, coplanar waveguides have the advantage of being simple to integrate with active devices. The literature outlines a variety of feeding techniques. Shilpee et al. [30] studied feeding strategies for single-layer PCB antennas using coplanar waveguides, particularly inductive or capacitive coupling through slots. Furthermore, because the coplanar waveguide (CPW) conductor acts as a ground plane for the patch, typical aperture coupling does not require a feed substrate.

* Corresponding Author.
Email: nurulfahmi@upi.edu
Received: January 04, 2023 ; Revised: February 27, 2023
Accepted: May 11, 2023 ; Published: August 31, 2023

Open access under CC-BY-NC-SA
© 2023 BRIN

Important research topics include reconfiguration, tuneability, and increasing bandwidth without reducing excess PCB antennas. The most often utilized strategies for enhancing the operating frequency of antennas include the employment of parasitic patches in single-layer and multilayer designs [31], the use of foam or air substrates [32], [33], and the addition of slots in the patch, including a U-patch antenna [34]. On the other hand, using a parasitic patch will change the dimension of the PCB antenna [35]. Furthermore, increasing the thickness of the substrate or using a multilayer produces a more substantial surface wave, which reduces efficiency. Although U-slot antennas and similar specifications have a wide operating frequency range, they cannot be reconfigured.

SDR devices like HackRF require wideband antennas that can match the working frequency. However, current research on antennas for SDR has resulted in a narrow operational frequency. For instance, Devi et al. [36] created a CPW antenna for SDR, but the frequency obtained only ranges from 2.4 GHz to 5 GHz. Likewise, Patron [37] designed an antenna for SDR by adding a diode component with an operating frequency range of 2 GHz to 3 GHz. Ibrahim et al. [38] Designing a microstrip antenna for spectrum sensing using an SDR platform as a receiver. The antenna is made as a microstrip with dimensions of 80 mm × 60 mm. The designed antenna was successfully integrated with SDR to test the spectrum sensing with a frequency range of 1.5 GHz– 2.8 GHz. The results of the antenna research for SDR are shown in Table 1.

Based on the discussion presented, this study aims to create a wideband microstrip CPW antenna for SDR that can be modified to achieve the desired operational frequency by adding an arm above the feed line. The results obtained from the simulation and fabrication of the antenna dimensions will be compared. The fabricated results will be implemented using HackRF as the SDR device, with performance testing at 2.4 GHz, 3 GHz, and 4 GHz frequencies using the ADF4351 signal generator. This paper will present the simulation and fabrication of antenna dimensions in section 2 and the influence of various antenna parameters in section 3. Section 3 will also compare the simulation and antenna measurements' radiation pattern and current distribution. Finally, section 4 will provide conclusions based on the results obtained in this study.

II. COPLANAR WAVEGUIDE ANTENNA DESIGN

CPW is part of the transmission line as a feeder for microstrip antennas that can carry electric current [39]. CPW consists of one conductor as a medium for electric current to flow to a patch printed on the dielectric material and followed by two conductors as a ground which has a CPW schematic distance as shown in Figure 1. The CPW impedance can be calculated using (1)–(6), for the length of the CPW feed line it can be calculated using equation (7).

$$k = \frac{a}{b} \tag{1}$$

$$k' = \sqrt{1 - k^2} \tag{2}$$

$$k_l = \frac{\tanh\left(\frac{\pi a}{4h}\right)}{\tanh\left(\frac{\pi b}{4h}\right)} \tag{3}$$

$$k_l' = \sqrt{1 - k_l^2} \tag{4}$$

$$\varepsilon_{cpw} = \frac{1+\varepsilon_r \frac{K(k')K(k_l)}{K(k)K(k_l')}}{1+\frac{K(k')K(k_l)}{K(k)K(k_l')}} \tag{5}$$

$$Z_o = \frac{60\pi}{\sqrt{\varepsilon_{eff}}} \frac{1}{\frac{K(k')K(k_l)}{K(k)K(k_l')}} \tag{6}$$

$$L_f = 0.537\lambda_g \tag{7}$$

The radiating element serves the purpose of emitting both magnetic and electric waves. These radiating patches are usually made up of conducting layers of different thicknesses, and they come in various forms, such as circular, triangular, rectangular, and others. The fabricated antenna dimensions are shown in Figure 2, while the antenna fabrication is shown in Figure 3. The fundamental shape of a patch antenna is circular, but the top patch is altered to resemble a flower shape. An arm with a 1 mm width is added to the center of the antenna. The antenna feedline, which has a width of 2.75 mm, is situated between the ground planes, and its distance from both ground planes is 0.38 mm. During antenna fabrication, it is necessary to consider the feedline distance from the ground plane since it can cause radiation leakage. The size and position of the feedline and arm patch will be examined to determine their impact on the antenna's performance. CST Studio Suite software was used to design the antenna, as shown in Figure 2. Several optimizations were carried out in the simulation process to obtain results according to specifications. The antenna uses a 0.8 mm FR-4 substrate with a permittivity of $\varepsilon_r = 4.3$. The fabricated antenna is shown in Figure 2.

The antenna design process uses several equations to determine the variables, such as characteristic impedance and effective permittivity [18]. The equation for the antenna dimensions is also used as a basic reference in the design. As the feed to the SMA connector, the

TABLE 1
SUMMARY OF 3 ANTENNA FOR SDR APPLICATION

Literature work	Antenna type	Frequency (GHz)	Bandwidth (MHz)
Devi et al. [36]	Microstrip patch antenna	2.38–2.52	140
Patron [37]	Microstrip patch antenna	2.4–3	600
Ibrahim et al. [38]	Microstrip patch antenna	1.5–2.8	1300

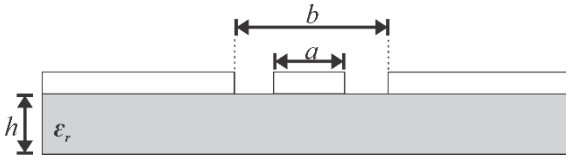

Figure 1. The coplanar waveguide structure.

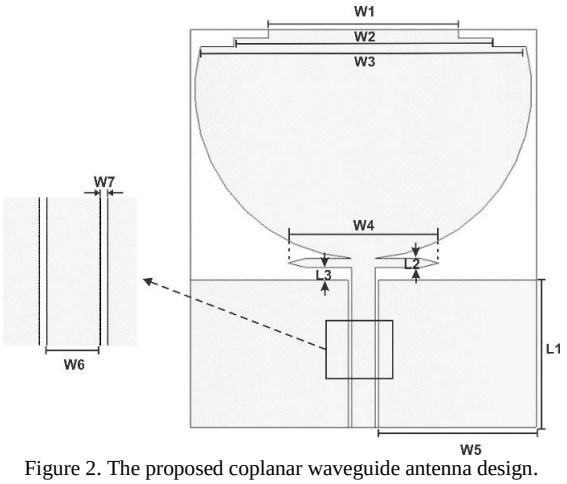

Figure 2. The proposed coplanar waveguide antenna design.

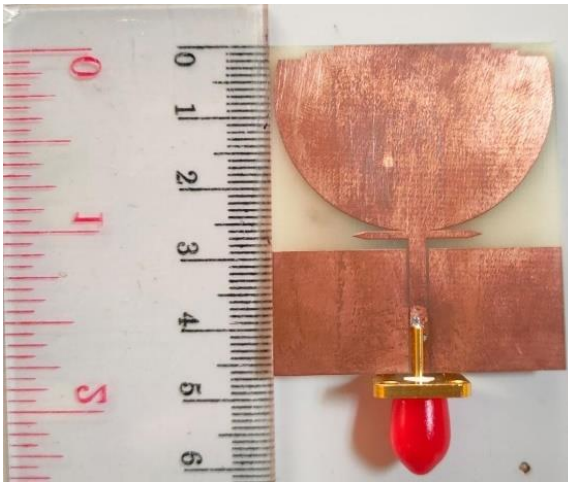

Figure 3. The fabricated coplanar waveguide antenna.

antenna impedance uses the 50 Ω microstrip line method. Table 2 shows the CPW antenna's structure. The antenna design has dimensions of 40 mm × 46 mm × 0.8 mm.

III. Simulation and Measurement Results

This section will examine the impact of each proposed antenna parameter, which can help broaden the antenna design process. The CST Studio Suite was used to conduct and evaluate parametric studies. Various design steps were taken to arrive at the final design of the proposed UWB antenna, including the analysis of important parameters.

A. Analyzing important parameters through parametric studies

The first variable to be observed is the feed line width (W6) of the antenna. The antenna feed line width is simulated from 2 mm to 3 mm, as shown in Figure 4. The simulation results indicate that the resonant frequency moves to a lower frequency. When the feed line width is 2 mm, the lowest frequency of the antenna is at 2.35 GHz, and the upper frequency of the antenna is at 6.45 GHz. This feed line width can be optimized to obtain proper coupling from the feed line to the patch antenna. Furthermore, the feed line width is changed to 2.25 mm. The results obtained are better than the previous feed line width. The lower frequency of the antenna shifts to a lower frequency at 2.1 GHz, and the upper frequency is at 6.45 GHz.

Table 2
Antenna Parameters

Parameters	Dimensions (mm)
L1	17
L2	1
L3	1.5
W1	22
W2	30
W3	37.7
W4	17.5
W5	18.25
W6	2.75
W7	1.75

The antenna's resonant frequency moves lower when the feed line width is increased. It can be seen that when the feed line width is changed to 3 mm, the lower frequency of the antenna can reach 1.96 GHz. However, it has an impact on the value of the reflection coefficient. The feed line width with a value of 3 mm increases to -10 dB at 3 GHz. At a frequency of 3 GHz, the feed line width of 2 mm to 2.75 mm has a reflection coefficient of less than -10 dB. The simulation results show that the width of the feed line affects impedance matching. The lower the resonant frequency of the antenna moves to the left as the feed line width increases.

The second variable observed is the antenna arm (W4) which is above the feed line. The results of the optimization of the antenna arm are shown in Figure 5. The antenna arm length is simulated with various values from 2.5 mm to 10 mm. The antenna arm with a length of 2.5 mm has a bandwidth range of 1.9 GHz–5.5 GHz. The antenna arm with a length of 4.5 mm has a bandwidth range of 1.9 GHz–5.8 GHz. The 6.75 mm long antenna arm has a bandwidth range of 1.9 GHz–6.4 GHz. The simulation results demonstrate that the resonant frequency value of the antenna moves to the right when optimization is carried out from 2.5 mm to 6.7 mm. The maximum resonant frequency of the antenna moves to the left when the antenna arm is 9 mm to 10 mm long.

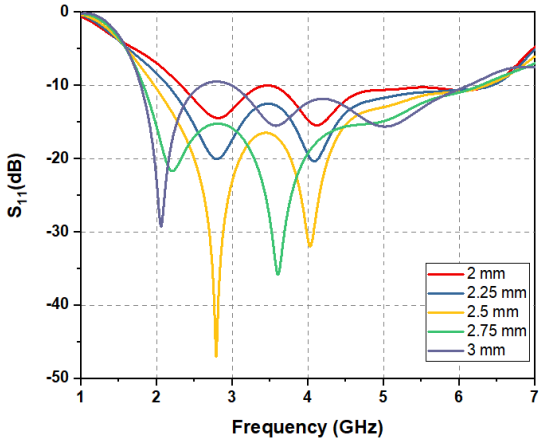

Figure 4. The simulated effect of feed line width (W6) on antenna reflection coefficient.

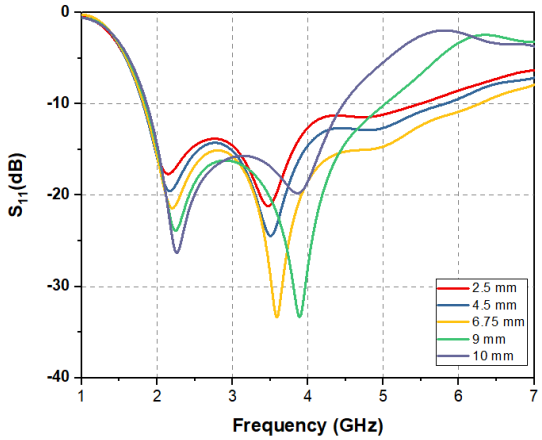

Figure 5. The simulated effect of the antenna arm (W4) on return loss.

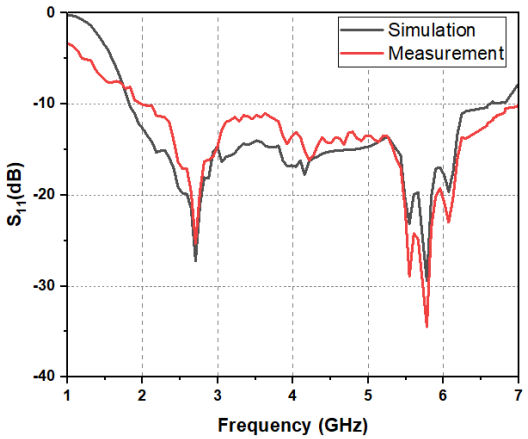

Figure 7. The comparison of simulated and measured return loss.

The impact of this top frequency move makes the antenna bandwidth narrower, namely 1.9GHz–5GHz and 1.9GHz–4.5GHz.

Based on the results obtained, changes in the length of the antenna arm can affect the resonant frequency. The reflection coefficient of the antenna has a particular optimum distance when the arm length is changed. The length of the antenna arm, which is 2.5 mm to 6.75 mm, makes the upper resonant frequency of the antenna shift to the right. This resonant frequency shift makes the antenna bandwidth wider. However, the upper resonant frequency of the antenna shifts to the left when the arm length of the antenna is more than 6.75 mm. The shift is because the current is strongly distributed in the feed line. The parameter W7 influences the antenna performance, as shown in Figure 6. This variable is adjusted such that the ground plane has no effect on the ideal coupling from the feed line to the patch. According to the W7 optimization, 1.75 mm is the ideal distance between the feed line and the antenna ground plane. Consequently, the spacing between the feed line and the ground plane has a major impact on the resonance frequency and bandwidth of the antenna.

B. Return Loss

The return loss comparison between the results from simulation and measurement is shown in Figure. 7. The return loss characteristics were measured with a network analyzer. The measured return loss graph shows an antenna operating frequency of less than -10 dB from 2 GHz to 7 GHz, whereas the simulation results show an antenna operating frequency ranging from 1.8 GHz to 6.5 GHz.

Several factors could be responsible for the discrepancy between the simulated and measured results. These factors may include the inappropriate standard dielectric constants used in both the simulation and fabrication processes and errors that may occur during the measurement process. Despite this, the difference remains within acceptable limits, since the operational frequency of the antenna still meets the specifications of the SDR utilized.

C. The radiation pattern of the proposed work

The antenna radiation pattern is shown in Figure 8, Figure 9, and Figure 10. Around 2–4 GHz, the antenna emits an omnidirectional radiation pattern in the E-plane. The experimental results show a reasonably good match with the simulation. The proposed antenna has the same radiation pattern at 2–4 GHz frequency. The antenna has omnidirectional radiation, which means it can receive signals from all directions. The radiation pattern is also influenced by the antenna's ground plane. The antenna radiation pattern is symmetrical because it has identical ground plane dimensions surrounding the feeding point.

D. Current distribution

As shown in Figures 11, Figure 12, and Figure 13, the simulation result of electric current distribution is found on the top border of the ground plane, the bottom of the patch, the outside edge of the patch, the patch arm,

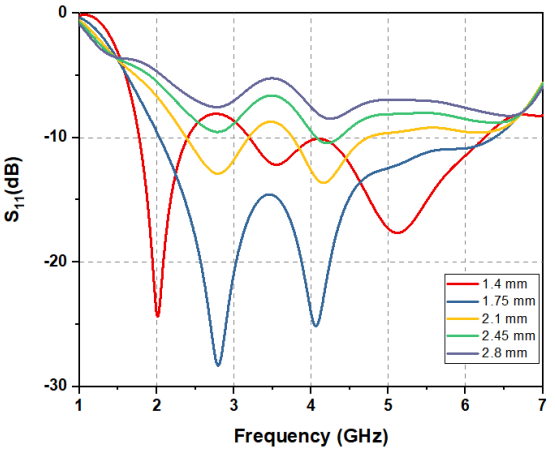

Figure 6. The simulated effect of the antenna arm (W7) on return loss.

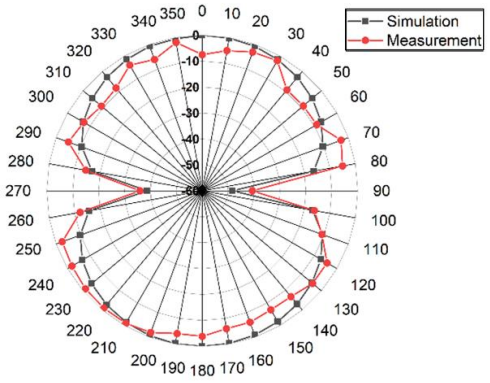

Figure 8. The simulated and measured patterns of the normalized E-field antenna radiation at 2 GHz.

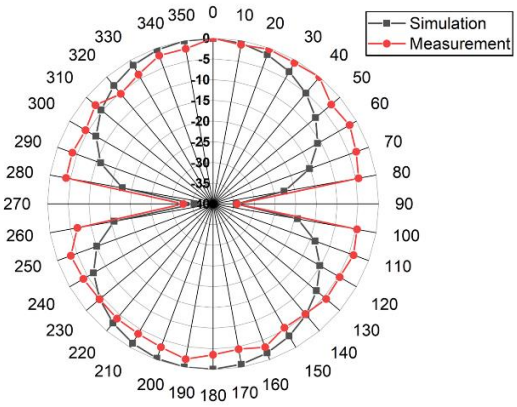

Figure 9. The simulated and measured patterns of the normalized E-field antenna radiation at 3 GHz.

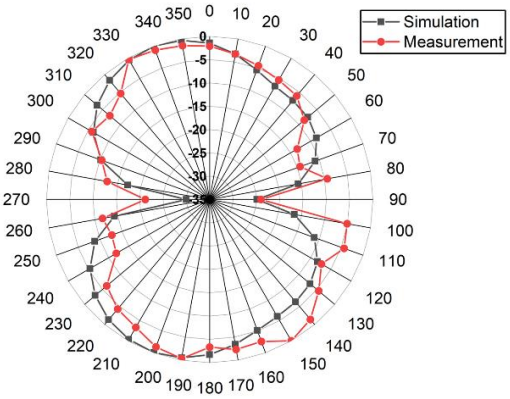

Figure 10. The simulated and measured patterns of the normalized E-field antenna radiation at 4 GHz.

and the feed line. At the same frequency, the current is distributed at the center of the antenna's feed. The current distribution at the ground plane implies that the portion of the ground plane closest to the patch functions as part of the radiation structure. As a result, the distance between the patch arm and the ground plane substantially impacts antenna return loss. In a symmetrical E-plane, the x-field components on the right and left sides of the patch are pointing in opposing directions and will cancel each other out in the far field. This x-field component also generates a cross-polarized pattern in the H-plane.

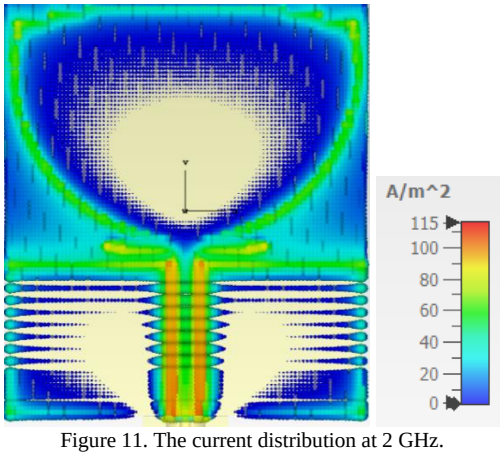

Figure 11. The current distribution at 2 GHz.

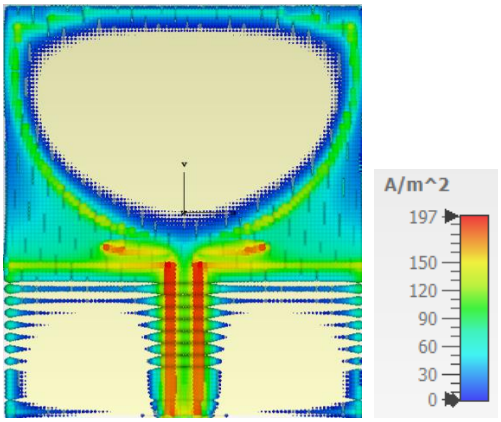

Figure 12. The current distribution at 3 GHz.

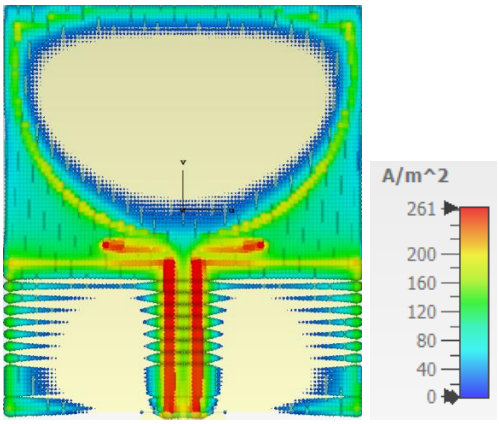

Figure 13. The current distribution result at 4 GHz.

E. Gain

The antenna gain comparison is shown in Figure 14. The simulated gain results increase with increasing the frequency up to 6 GHz. The lowest gain value is at the 2 GHz frequency, 2.1 dB. The measurement yielded similar results to the simulation of the antenna gain. The measured gain values at some frequencies are lower, and some are higher than the simulated gain. The measured gain reaches 2.5 dB at a frequency of 2 GHz, while in the simulation the gain is 2.08 dB. Furthermore, at a frequency of 3 GHz, the measured gain reaches 3.21 dB, while the simulated gain is only 3 dB. At 4 GHz

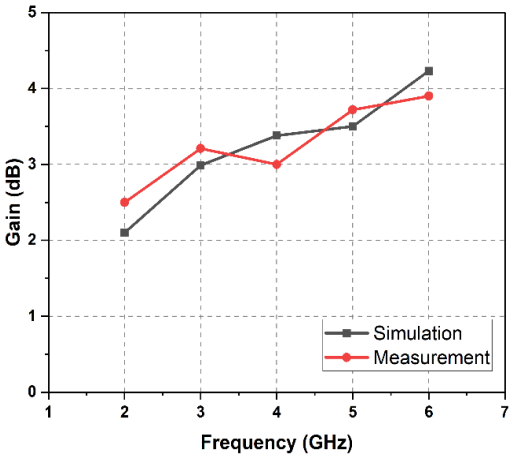

Figure 14. The comparison of simulated and measured gains of the proposed antenna.

frequency, the simulated gain is greater than the measured gain; the simulated gain is 3.3 dB, while the measured gain is 3 dB. The simulated gain at 5 GHz frequency is 3.5 dB, while the measured gain is 3.6 dB. The highest gain from the simulation and measurement results is at the 6 GHz frequency. The gain of the simulation results obtained is 3.92, while the gain of the measurement results is 4.2 dB.

F. HackRF Implementation

Antenna implementation was conducted using a signal generator and HackRF. The antenna was positioned as a transmitter and receiver. The antenna test design is shown in Figure 15. The signal transmitter uses the ADF4351 signal generator capable of generating signals up to 4 GHz frequencies. The signal generator was connected to the antenna and placed in room 1. HackRF was used at the receiver, capable of receiving signals up to 6 GHz. HackRF was connected to the receiving antenna and placed in a different location from the transmitter. The distance between the receiver and transmitter was 10 m.

The GNURadio software was used to view the signals received from HackRF. The block diagram used in GNURadio is shown in Figure 16. The block diagrams were “osmocom source” and “WX GUI FFT Sink”. The “osmocom source” block is used for SDR hardware such as HackRF. The configuration in this block is the sample rate the number of samples per second. The center frequency is the frequency that is tuned to the radio frequency (RF). The frequency correction factor is in parts per million (ppm) and can be set to 0 if it is unknown. The DC offset mode controls the hardware DC offset. The DC offset function can only be used on the USRP. The IQ balance mode was used to control the software IQ imbalance correction. The gain mode was used to select between the manual (default) and automatic gain mode as appropriate. The RF gain is the overall RF gain of the device. The IF gain is the overall

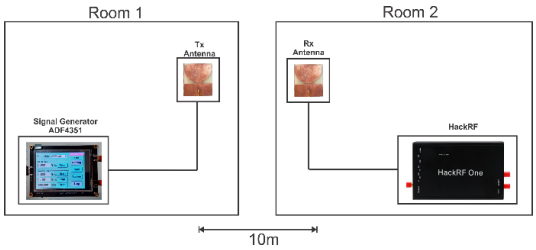

Figure 15. The implementation of the proposed antenna.

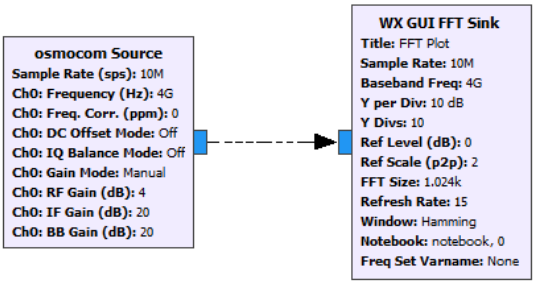

Figure 16. The GNURadio block diagram.

intermediate frequency gain of the device. This setting is available for the RTL-SDR and the OsmoSDR devices with the E4000 and the HackRF tuners in the transmitter and receiver mode. The BB gain is the overall baseband gain of the device. This setting is available for HackRF in the receiver mode. Observations lead to a reasonable gain range from 15 to 30 dB.

The implementation process included testing the antenna by receiving signals at 2.4 GHz, 3 GHz, and 4 GHz frequencies. Based on the results obtained, the fabricated antenna can receive signals from the transmitter. As can be seen in Figure 17, Figure 18, and Figure 19, there is a higher peak power compared to other frequencies at each of the 2.4 GHz, 3 GHz, and 4 GHz frequencies.

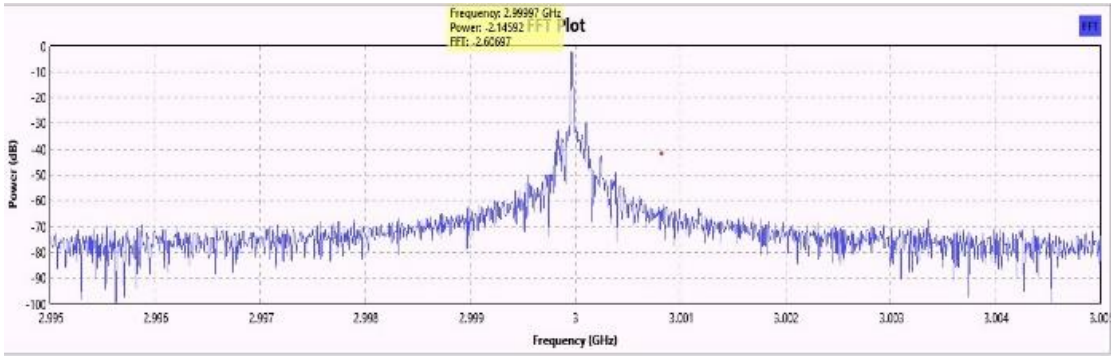

Figure 17. The received signal at frequency 2.4 GHz.

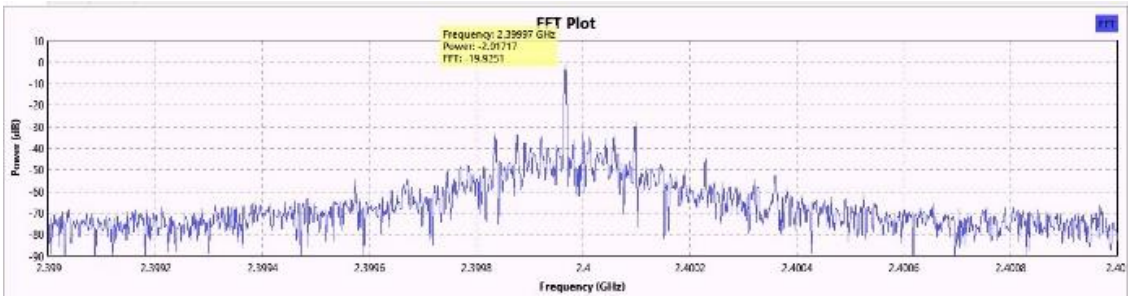

Figure 18. The received signal at frequency 3 GHz.

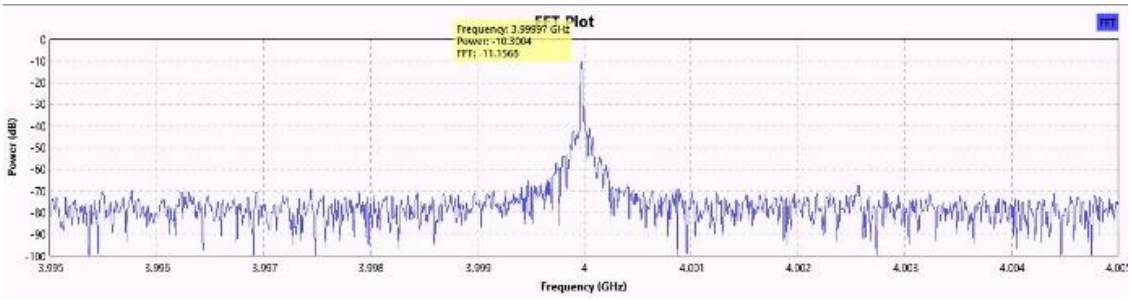

Figure 19. The received signal at frequency 4 GHz.

IV. CONCLUSION

Compact planar antennas are provided for software-defined radio. The proposed antenna has been optimized through simulation and fabricated with a compact size of 40 mm × 46 mm × 0.8 mm. Antenna geometric parameters such as feed line width, antenna arm, and distance between the feed line and ground plane are examined to identify the best design Antenna return loss measurements using VNA show that the antenna can operate at a frequency of 2 GHz to 6 GHz. The measurement findings demonstrate a discrepancy between the simulation and measurement results for antenna return loss. The antenna's operational frequency from the simulation is 2 GHz–6.5 GHz, but its operational frequency from the measurement is 2 GHz–7 GHz. At 2 GHz–4 GHz, the antenna radiation pattern is omnidirectional. CPW antennas are suitable for SDR because of their compact size and appropriate bandwidth. Antenna fabrication results have been successfully implemented in SDR. The antenna has been used as a transmitting and receiving medium at 2.4 GHz, 3 GHz, and 4 GHz. In the implementation that has been done, the antenna can receive the signal emitted from the signal generator.

DECLARATIONS

Conflict of Interest

The authors have declared that no competing interests exist.

CrediT Authorship Contribution

Nurul Fahmi Arief Hakim: Conceptualization, Methodology, Software, and Validation; Silmi Ath Thahirah Al Azhima: Data curation, Writing-Original draft preparation; Mariya Al Qibtiya: Writing-Reviewing and Editing.

Funding

This work was supported by UPI research program (Penelitian Afirmasi) under contract number 906/UN40/PT.01.02/2023.

Acknowledgment

The authors are grateful to Coplanar Waveguide and Microcontroller research group Universitas Pendidikan Indonesia in the software-defined radio project for supporting this research.

REFERENCES

[1] Y. Dou, Z. Chen, J. Bai, Q. Cai, and G. Liu, "Two-port CPW-fed dual-band MIMO antenna for IEEE 802.11 a/b/G applications," *Int. J. Antennas Propag.*, vol. 2021, Jun. 2021, Art. No. 5572887, doi: 10.1155/2021/5572887.

[2] A. H. Ilyasah, M. Hidayat, and S. U. Prini, "2×1 truncated corner microstrip array antenna to increase gain and bandwidth for LTE applications at 2.3 GHz frequency," *J. Elektr. Telekom.*, vol. 22, no. 1, pp. 14–22, Aug. 2022, doi: 10.55981/jet.436.

[3] J. Wang, H. Wong, Z. Ji, and Y. Wu, "Broadband CPW-fed aperture coupled metasurface antenna," *IEEE Antennas Wirel. Propag. Lett.*, vol. 18, no. 3, pp. 517–520, Mar. 2019, doi: 10.1109/LAWP.2019.2895618.

[4] T. Liu, Y. Sun, J. Li, J. Yu, and K. Wang, "CPW- fed compact multiband monopole antenna for WLAN/WiMAX /X-Band application," *Prog. Electromagn. Res. Lett.*, vol. 87, pp. 105–113, Oct. 2019, doi: 10.2528/PIERL19080902.

[5] F. Ouberri, A. Tajmouati, I. Zahraoui, A. Lakhssassi, M. Latrach, and R. Er-Rebyiy, "A novel wideband cpw-fed square aperture monopole antenna with inverted-l grounded strips for wireless and satellite applications," in *Proc. 2020 IEEE 2nd Int. Conf. on Electron., Control, Optim. And Comput. Sci. (ICECOCS)*, Dec. 2020, doi: 10.1109/ICECOCS50124.2020.9314499.

[6] S. Ullah, I. Ahmad, Y. Raheem, S. Ullah, T. Ahmad, and U. Habib, "Hexagonal shaped CPW Feed based Frequency Reconfigurable Antenna for WLAN and Sub-6 GHz 5G applications," in *Proc. 2020 Int. Conf. Emerging Trends in Smart Technol. (ICETST)*, Apr. 2020, doi: 10.1109/ICETST49965.2020.9080688.

[7] K. -L. Wong, H. -J. Chang, C. -Y. Wang, and S. -Y. Wang, "Very-low-profile grounded coplanar waveguide-fed dual-band WLAN slot antenna for on-body antenna application," *IEEE Antennas Wirel. Propag. Lett.*, vol. 19, no. 1, pp. 213–217, Jan. 2020, doi: 10.1109/LAWP.2019.2958961.

[8] K.-L. Wong, *Compact and Broadband Microstrip Antennas*. New York, NY, USA: J. Wiley, 2002.

[9] U. L. Rohde, J. C. Whitaker, and H. Zahod, *Communications Receivers: Principles and Design*. New York, NY, USA: McGraw-Hill, 2018.

[10] N. F. A. Hakim and I. Kustiawan, "Experimental study of FM complex differentiation using HackRF," in *Proc. 2021 Int. Res. Symp. Adv. Eng. And Vocational Educ. (IRSAEVE)*, Nov. 2021, pp. 10–13, doi: 10.1109/IRSAEVE52613.2021.9604018.

[11] I. Martoyo, P. Setiasabda, H. Y. Kanalebe, H. P. Uranus, and M. Pardede, "Software defined radio for education: spectrum analyzer, FM receiver/transmitter and GSM sniffer with HackRF One," in *Proc. 2018 2nd Borneo Int. Conf. Appl. Math. And Eng. (BICAME)*, Dec. 2018, pp. 188–192, doi: 10.1109/BICAME45512.2018.1570509150.

[12] G. Avdeyenko, "Application of Nuand BladeRF x40 SDR Transceiver for Generating Television Signals of DVB-S2 Standard," in *Proc. 2019 Int. Conf. Inf. And Telecommun. Technol. And Radio Electron. (UkrMiCo)*, Sep. 2019, doi: 10.1109/UkrMiCo47782.2019.9165515.

[13] R. Glazkov, D. M. Yurackov, and V. V. Moshkov, "GNU Radio Based RDS Transceiver for Data Communication," in *Proc. 2020 IEEE Conf. Russian Young Researchers Electrical and Electron. Eng. (EIConRus)*, Jan. 2020, pp. 21–23, doi: 10.1109/EIConRus49466.2020.9039319.

[14] A. Martian, C. Vladeanu, and I. Marghescu, "Novel software defined radio testbed for spectrum occupancy measurements," in *Proc. 2020 Int. Symp. Electron. And Telecom. (ISETC*), Nov. 2020, pp. 1-4, doi: 10.1109/ISETC50328.2020.9301075.

[15] M. B. Khan, M. Rehman, A. Mustafa, R. A. Shah, and X. Yang, "Intelligent non-contact sensing for connected health using software defined radio technology," *Electronics*, vol. 10, no. 13, Jun. 2021, Art. No. 1558, doi: 10.3390/electronics10131558.

[16] V. Dear, A. Purwono, I. Iskandar, A. Kurniawan, and P. Abadi. "Design of sliding correlator channel sounder for ionospheric channel probing based on software define radio." *Buletin Pos dan Telekomunikasi*, vol. 19, no. 1, pp. 1-14, Sep. 2021, doi: 10.17933/bpostel.2021.190101.

[17] T. Puklibmoung and W. Sa-Ngiamvibool, "Design and fabrication of broad-beam microstrip antenna using parasitic patches and cavity-backed slot coupling," *Appl. Syst. Innov.*, vol. 5, no. 2, Feb. 2022, Art. no. 31, doi: 10.3390/asi5020031.

[18] M. Fartookzadeh and S. H. Mohseni Armaki, "Efficiency improvement and cross-polarization reduction of single-fed frequency-scan leaky wave microstrip antennas by using an M-shape metasurface as the WAIM Layer," *AEU - Int. J. Electron. Commun.*, vol. 116, Mar. 2020, Art. no. 153057, doi: 10.1016/j.aeue.2019.153057.

[19] M. M. Alam, R. Azim, N. M. Sobahi, A. I. Khan, and M. T. Islam, "A dual-band CPW-fed miniature planar antenna for S-, C-, WiMAX, WLAN, UWB, and X-band applications," *Sci. Rep.*, vol. 12, May 2022, Art. no. 7584, doi: 10.1038/s41598-022-11679-7.

[20] J. M. Percaz et al., "Producing and exploiting simultaneously the forward and backward coupling in EBG-assisted microstrip coupled lines," *IEEE Antennas Wirel. Propag. Lett.*, vol. 15, pp. 873–876, Sep. 2015, doi: 10.1109/LAWP.2015.2478595.

[21] C. Zebiri et al., "Aperture-coupled asymmetric dielectric resonator antenna with slotted microstrip line for enhanced ultrawideband," in *Proc. 2016 10th European Conf. Antennas and Propag. (EuCAP*), Apr. 2016, doi: 10.1109/EuCAP.2016.7481393.

[22] A. R. Anu, P. Abdulla, T. K. Rekha, A. Iqubal, U. S. Kollannore, and P. M. Jasmine, "Bandwidth Enhancement of Aperture Coupled Cylindrical Dielectric Resonator Antenna using Modified Feed Structure," *in Proc. 2019 IEEE Region 10 Conf. (TENCON)*, Oct. 2019, pp. 1910–1912, doi: 10.1109/TENCON.2019.8929466.

[23] A T. Yasin and R. Baktur, "Bandwidth enhancement of meshed patch antennas through proximity coupling," *IEEE Antennas Wirel. Propag. Lett.*, vol. 16, pp. 2501–2504, Jul. 2017, doi: 10.1109/LAWP.2017.2726562.

[24] R. Del-Rio-Ruiz, J. -M. Lopez-Garde, J. Legarda, O. Caytan, and H. Rogier, "A combination of transmission line models as design instruments for electromagnetically coupled microstrip patch antennas in the 2.45 GHz ISM band," *IEEE Antennas Wirel. Propag. Lett*., vol. 69, no. 1, pp. 550–555, Jan. 2021, doi: 10.1109/TAP.2020.3001668.

[25] A. Ullah, N. O. Parchin, R. A. Abd-Alhameed, and P. S. Excell, "Coplanar waveguide antenna with defected ground structure for 5G millimeter wave communications," in *Proc. 2019 2nd IEEE Middle East and North Africa COMMun. Conf*., Nov. 2019, pp. 1-4, doi: 10.1109/MENACOMM46666.2019.8988584.

[26] H. S. N. Rahkmi, S. A. T. Al Azhima, M. Al Qibtiya, and N. F. A. Hakim, "Modification of CPW antenna using various slot shapes for wireless communication system," in *Proc. 2022 Int. Conf. Comput. Eng. Netw. and Intell. Multimedia (CENIM)*, Nov. 2022, pp. 317–320, doi: 10.1109/CENIM56801.2022.10037289.

[27] Y. Zhang, S. Li, Z. Q. Yang, X. Y. Qu, and W. H. Zong, "A coplanar waveguide-fed flexible antenna for ultra-wideband applications," *Int. J. RF Microw. C. E.*, vol. 30, no. 8, Aug. 2020, Art. no. e22258, doi: 10.1002/mmce.22258.

[28] M. Cetin and L. Alatan, "A novel input impedance computation method for coaxial probe fed microstrip antennas by utilizing characteristic modes," in *Proc. 2017 IEEE Int. Symp. Antennas and Propag. & USNC/URSI Nat. Radio Sci. Meeting*, Jul. 2017, pp. 947–948, doi: 10.1109/APUSNCURSINRSM.2017.8072516.

[29] J. Sun and K. -M. Luk, "A fully transparent wideband water patch antenna with L-shaped feed," *IEEE Open J. Antennas Propag.*, vol. 2, pp. 968–975, Sep. 2021, doi: 10.1109/OJAP.2021.3111700.

[30] S. Patil, A. K. Singh, B. K. Kanaujia, and R. L. Yadava, "Design of inclined coupling slot loaded CPW-fed circularly polarized slot antenna for wireless applications," *Electromagnetic*s, vol. 38, no. 4, pp. 226–235, Mar. 2018, doi: 10.1080/02726343.2018.1457270.

[31] D. G. Fang, *Antenna Theory and Microstrip Antennas.* CRC Press, 2019.

[32] A. Munir, I. Novianti, and B. Hasanah, "Experimental investigation of ADM-based microstrip square patch antenna with resonant frequency lowering characteristic," in *Proc. 2020 Int. Workshop Antenna Technol. (iWAT*), Feb. 2020, pp. 89-92, doi: 10.1109/iWAT48004.2020.1570615575.

[33] M. Gupta, S. Sachdeva, N. K. Swamy, and I. P. Singh, "Rectangular microstrip patch antenna using air as substrate for S-band communication," *J. Electromagn. Anal. Appl.*, vol. 06, no. 03, pp. 38–41, Feb. 2014, doi: 10.4236/jemaa.2014.63006.

[34] M. Khan and D. Chatterjee, "Characteristic mode analysis of a class of empirical design techniques for probe-fed, U-slot microstrip patch antennas," *IEEE Trans. Antennas Propag.*, vol. 64, no. 7, pp. 2758–2770, Jul. 2016, doi: 10.1109/TAP.2016.2556705.

[35] P. Mathur, M. Chattopadhyay, and G. Kumar, "Non-radiating edge gap coupled capsule-shaped and nose-shaped microstrip antennas for 3G applications," *Int. J. Future Comput. Commun.*, vol. 3, no. 2, pp. 80–83, Apr. 2014, doi: 10.7763/IJFCC.2014.V3.272.

[36] Devi, P. Kalapna, and Aparna Shekar, "Design of frequency reconfigurable antenna for SDR application," in *Proc. 2020 7th Int. Conf. Smart Struct. and Syst. (ICSSS)*, Jul. 2020, pp. 1-5, doi: 10.1109/ICSSS49621.2020.9202201.

[37] D. Patron and K. R. Dandekar, "Planar reconfigurable antenna with integrated switching control circuitry," in *Proc. 8th European Conf. Antennas and Propag. (EuCAP 2014)*, Apr. 2014, pp. 2737–2740, doi: 10.1109/EuCAP.2014.6902391.

[38] A. A. Ibrahim, W. A. E. Ali, and H. Aboushady. "Performance evaluation of SDR blade RF using wide-band monopole antenna for spectrum sensing applications," *Appl. Comput. Electromagn. Soc.*, vol. 36, no. 4, pp. 419–424, Apr. 2021, doi: 10.47037/2020.ACES.J.360407.

[39] K. L. Chung, H. Tian, S. Wang, B. Feng, and G. Lai. "Miniaturization of microwave planar circuits using composite microstrip/coplanar-waveguide transmission lines," *Alex. Eng. J.*, vol. 61, no. 11, pp. 8933–8942, Nov. 2022, doi: 10.1016/j.aej.2022.02.027.